

Article

Analysis of Dynamic Response and Ultimate Strength for Box Girder under Bending Moment

Gui-Jie Shi ^{1,2} , De-Yu Wang ^{1,2,*}, Fu-Hua Wang ³ and Shi-Jian Cai ³

¹ State Key Laboratory of Ocean Engineering, Shanghai Jiao Tong University, Shanghai 200240, China

² Institute of Marine Equipment, Shanghai Jiao Tong University, Shanghai 200240, China

³ Marine Design & Research Institute of China, Shanghai 200011, China

* Correspondence: dywang@sjtu.edu.cn

Abstract: The box girder can be seen as a kind of simplified ship structure that can withstand a vertical bending moment. Dynamic loads play an important role in structural safety analysis, such as ship bow slamming during harsh sea conditions. In this paper, the dynamic elastic–plastic response and ultimate strength of a box girder under a bending moment are analyzed. A box girder with the same cross-section scantlings and span length as the Nishihara experiment is selected as the analysis object. Based on the model experiment results, the non-linear FE analysis method is validated to capture the ultimate strength of a box girder under bending moment. Then, six box girders were designed to study the critical influence factors on the dynamic ultimate moment, including the model length, plate thickness, mass density and load excitation period. On the basis of structural dynamic response, an evaluation criterion of dynamic limit state for the box girder under a bending moment is proposed in this paper. Compared with the static ultimate moment, the change in the dynamic ultimate moment is discussed in detail to obtain the general principal method for dynamic strength analysis. The conclusions in this paper can provide guidance for dynamic ultimate strength evaluation.

Keywords: dynamic failure; dynamic ultimate strength; box girder; bending moment



Citation: Shi, G.-J.; Wang, D.-Y.; Wang, F.-H.; Cai, S.-J. Analysis of Dynamic Response and Ultimate Strength for Box Girder under Bending Moment. *J. Mar. Sci. Eng.* **2023**, *11*, 373. <https://doi.org/10.3390/jmse11020373>

Academic Editor: Erkan Oterkus

Received: 1 January 2023

Revised: 18 January 2023

Accepted: 4 February 2023

Published: 8 February 2023



Copyright: © 2023 by the authors. Licensee MDPI, Basel, Switzerland. This article is an open access article distributed under the terms and conditions of the Creative Commons Attribution (CC BY) license (<https://creativecommons.org/licenses/by/4.0/>).

1. Introduction

Recent catastrophic incidents involving large ships, such as the MSC Napoli report [1] and the MOL Comfort report [2], show that dynamic load conditions may be one of the causes of structural failure. At present, the ultimate strength of a hull girder is usually evaluated under static loading conditions, and some partial safety factors are introduced to cover the dynamic effect. The whipping response of large ships has a higher frequency than the ordinary wave response; hence, the dynamic effects may provide additional strength reserves for the ship structure [3]. A partial safety factor [4] of 0.9 is proposed to reduce the effectiveness of the whipping moment in the ultimate strength check. For the lateral dynamic load condition, the dynamic strength of the beam under lateral impact could reach up to 1.4 times that of the static strength [5]. There are some large differences related to the structural dynamic strength evaluation that require further study.

The dynamic ultimate hull girder strength of a container ship under bending moments was studied by using the non-linear FE method [6]. The ultimate rotation of the cross-section around the neutral axis was used as the evaluation criterion to estimate the dynamic ultimate strength. When the duration of the dynamic bending moment was close to the natural period of the hull girder, the maximum cross-section rotation response was 1.6 times greater than that of the same amplitude of a static bending moment. The dynamic collapse under a whipping moment for a container ship was studied [7–9] to find that the dynamic ultimate strength increased by 5.9–8.4% compared to the static conditions. Therefore, it is necessary to carry out more studies to find a reasonable justification for the evaluation criteria for dynamic strength.

Compared with static loading conditions, the inertia terms might not be negligible in the case of a dynamic response when the load duration time is shorter than the natural period of the box girder [10]. The inertia force along the beam was commonly assumed to be linear under dynamic conditions, as proposed by [11], which caused a time-varying bending moment distribution along the beam. When the load duration was very short, the box girder could not react immediately, and a time lag took place [12]. These time lags caused differences between the external applied bending moment and the internal bending moment.

For a simply supported beam [13], the beam initially deformed at the mid-span in the first impact stage, and thereafter, the impact effect propagated to the end supports. When the dynamic bending moment exceeds some degree, the beam exhibits part failures, such as plastic hinges [14]. The local failure might present during the dynamic load action period and also might present during the free vibration stage after the action of the dynamic loads [15]. It was useful to find the critical dynamic load, which induced severe damage, for the safety analysis of a box girder.

Based on the dynamic load application method, the dynamic model tests could be categorized into two categories: the water basin test and the drop hammer test. These tests can obtain the characteristics of the dynamic varying over time, which can be used to guide structural dynamic response analysis. The dynamic ultimate strength under an impact load will show the structural carrying capacity and failure mode.

In the water basin test, the girder structure should be simplified and have a lower capacity, which could be damaged by the hydrodynamic force due to basin waves. A one-degree-of-freedom beam model was used to simulate the bending stiffness and then study the collapse behavior under whipping loads by using a numerical method [16] and the water basin test [17].

The drop hammer test has often been used to study the dynamic capacity of different structures. Three-point bending tests [18] were carried out to study the dynamic and quasi-static bending behavior of thin-walled aluminum tubes. A series of drop-weight tests [19] were carried out for the double-hat structure under lateral impacts to show their crashworthiness performance. A series of repeated impact tests [20] were carried out for in situ prestressed concrete sleepers, ranging from a low drop height to the limit drop height, where the ultimate failure occurred.

Several buckling criteria were proposed to determine the dynamic critical load, such as the B-R criterion [21], the plate thickness criterion [22] and so on. The B-R criterion states that dynamic stability loss occurs when the maximum plate deflection grows rapidly at a small variation in the load amplitude. The plate thickness criterion states that the dynamic critical load corresponds to the amplitude of the impact load at which the maximum plate deflection was equal to 0.5~1 times plate thickness. The box girder had more complex structures and a stable post-buckling path. It was necessary to study the evaluation criterion applicable to the dynamic ultimate moment of the box girder.

In summary, there are some problems that require further study, including the increase in the dynamic ultimate moment compared with static conditions, the expression of the dynamic ultimate moment index, critical dynamic-moment-induced girder failure and the evaluation criterion applicable to the dynamic ultimate moment.

In this paper, the box girder with the same cross-section scantlings and span length as the experiment [23] was selected as the object of the analysis. Based on the non-linear FE method verified by experiment results, the dynamic ultimate bending moment and evaluation criterion are studied in detail. Then, the influence factors, including the model length, plate thickness, material density and load duration time, are discussed.

2. Scantlings of Box Girder with Stiffened Panel

2.1. Analysis Object

Stiffened panels are a kind of fundamental element involved in ship structures that can withstand in-plane loads and lateral loads. In the longitudinal direction, the length of a

stiffened panel between two neighboring strengthened transverse frames is a span. Several stiffened panels can be assembled to form a closed cross-section. The box girder is made of some spans of closed cross-sections with stiffened panels, which can withstand many types of applied loads, including the vertical bending moment perpendicular to the box girder length direction.

Box girders are also used in experimental research due to their rich mechanical properties and easy fabrication, which can be considered to be a representation of simplified hull girders. A series of model experiments [23] for eight box girders under static bending moments were carried out. These box girders have also been selected by other researchers to study the influencing factors that affect the ultimate strength, such as initial imperfections [24], pitting corrosion and cracking [25], and the modeling method in non-linear FE analysis [26].

One of these box girders in the experiment [23] named MST-3 was selected as the analysis object in this paper in order to study its dynamic ultimate strength. The choice of this frequently used model is convenient for showing the structural response differences between static and dynamic bending moments.

In the Nishihara experiment, four points bending facilities were used to simulate a vertical bending moment condition for the mid-span of the box girder. The mid-span is the critical focused area in the experiment. At each end, the box girder was placed on a foundation that had a round steel bar on its top. Two concentrated forces were applied by the load cell on the transverse frames of the two sides of the mid-span. The two forces were applied symmetrically and simultaneously on the transverse bulkheads, which were a certain distance from the mid-span of the box girder. Therefore, the middle part of the experiment would be under pure bending conditions. More details about the experiment can be found in the reference [23].

The cross-section and scantlings of box girder MST-3 are shown in Figure 1 and Table 1. The span length between the two neighboring transverse frames of the experiment model is 540 mm. The cross-section is a square with the same scantlings of stiffened panels on four boundaries. The thickness of the plating is 3.05 mm, which is not an integer due to the actual plate measurement. The height of the stiffener web is 50 mm. A mild steel is used in the box girder with a yield strength of 278 MPa. However, the initial imperfection of the MST-3 box girder has not been mentioned in the [23] experiment. Several amplitudes of initial imperfection should be analyzed in the following FE calculation.

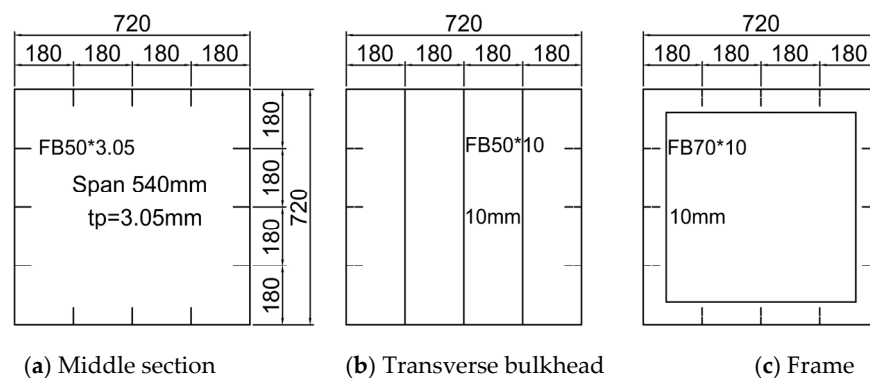


Figure 1. Cross-section of box girder MST-3 in the experiment [23]. (Span length = 540 mm; Plating thickness $t_p = 3.05$ mm; Stiffener $FB50 \times 3.05$; Stiffener spacing = 180 mm).

Table 1. Scantlings of box girder MST-3 in the experiment [23].

Member	Scantlings	Yield Strength	Modulus	Span
	mm	MPa	MPa	mm
Plating	3.05	287	2.07×10^5	540
Stiffener	50×3.05	287	2.07×10^5	540

2.2. Experiment Results under Static Bending Moment

In the experiment, the upper panel under compression showed a buckling mode with several half-waves. As the bending moment increased, the side shell started to present with buckling. At the limit state, the upper panel and side shell both presented a large buckling deformation, and the bottom presented a large tension stress but no fracture. The curve of Nishihara’s MST-3 model under a static bending moment is shown in Figure 2. The ultimate strength of the experiment model was about $M_{ult,s} = 5.88 \times 10^8$ Nmm. Based on the linear beam theory, the yield moment of the girder is $M_y = 7.03 \times 10^8$ Nmm, which corresponds to the first yield point at the deck farthest from the neutral axis. The full plastic moment of the girder is $M_p = 8.24 \times 10^8$ Nmm, which corresponds to the full yielding of the whole cross-section. The yielding moment M_y and the fully plastic moment M_p for this box girder are both larger than the ultimate bending moment of $M_{ult,s}$ obtained by the experiment. This is because the buckling strength is lower than the yielding strength of the material. Therefore, it is reasonable to use the ultimate strength in the safety assessment method.

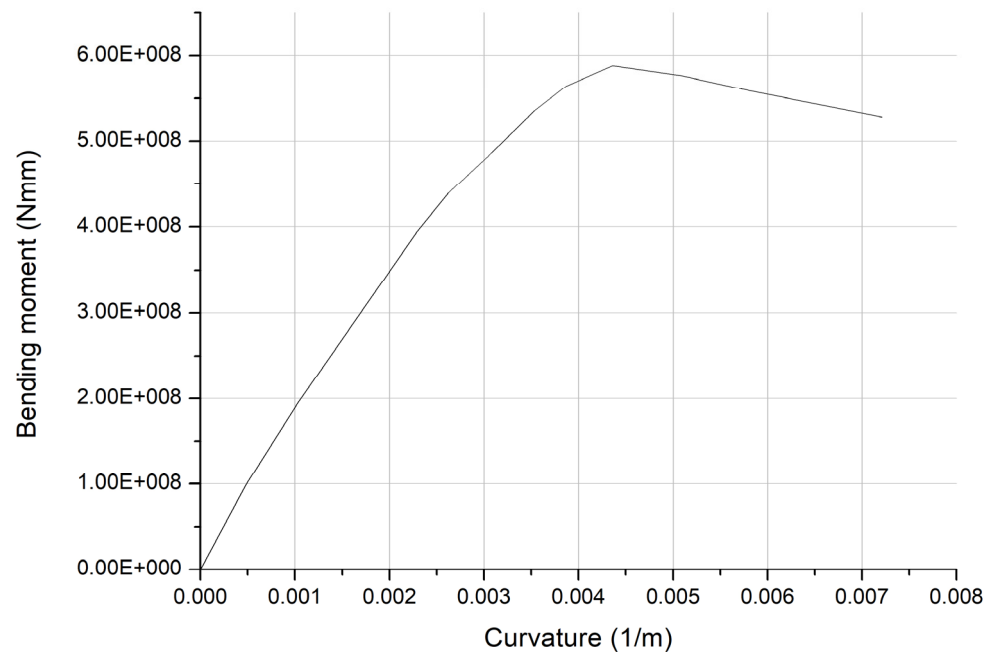


Figure 2. Load and curvature curve of box girder MST-3 under static bending moment in the experiment [23].

3. Non-Linear FE Analysis Method

The non-linear FE analysis method can be used to simulate the deformation failure process as the bending moment increases and obtain the ultimate strength of the bending moment by the extreme value of the load–deformation curve. Several parameters in the non-linear FE analysis, such as the boundary conditions, material properties, meshing density and imperfections, should be discussed and confirmed. The ABAQUS software is used in this paper.

3.1. Boundary Conditions and Loads

The coordinate system is defined as follows: X along the model length direction, Y along the model width direction, and Z along the model height direction.

The element type S4R for each element is chosen to simulate large deformation. This element has four nodes and six degrees of freedom in all nodes and a quadrilateral shape with reduced integration, hourglass control and a finite membrane strain.

The boundary conditions of the box girder are shown in Figure 3. The box girder model is assumed to be simply supported at the two ends. The aft end is constrained by the displacement degree of freedom $U_x = U_y = U_z = 0$ and the rotational degree of freedom $UR_x = UR_z = 0$ at the bottom edge. The fore-end is constrained by the displacement degree of freedom $U_y = U_z = 0$ and a rotational degree of freedom $UR_x = UR_z = 0$ at the bottom edge. Two forces, $F_1 = F_2$, along the vertical direction (Z axis), are applied as nodal forces on the upper edge of the bulkhead (BHD).

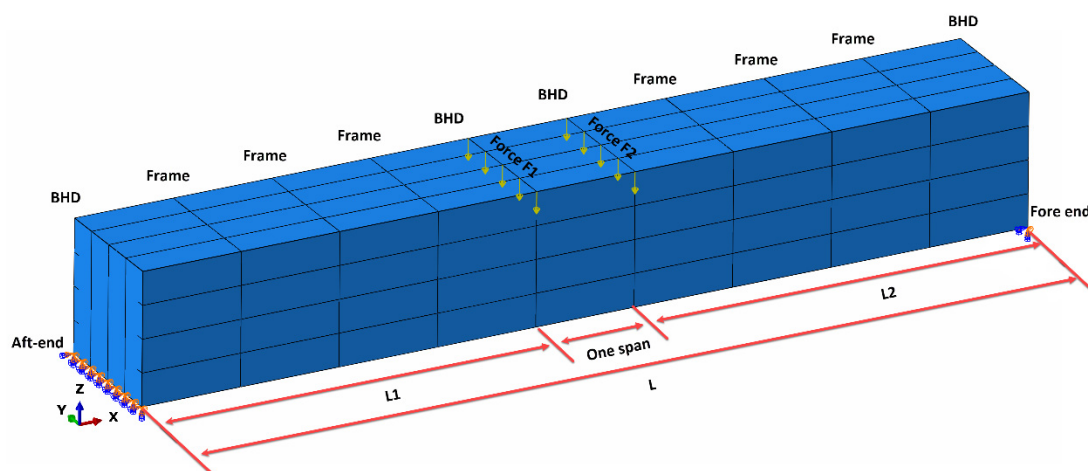


Figure 3. Boundary conditions of box girder.

The model width and height should include the whole section of the box girder. Usually, one-span or three-span are used to calculate the ultimate strength under static loading conditions. This paper will study the effect of more spans in the length direction on the dynamic ultimate strength.

3.2. Material Properties

As stated in the reference of [27], the yield strength for steel is usually higher than its nominal strength due to the positive tolerance measured by the tensile test results. The material properties based on the Nishihara test are used in this paper. The material of plates and stiffeners is modeled with Young’s modulus of $E = 206,000$ MPa, Poisson ratio $\nu = 0.3$ and yield strength of $\sigma_Y = 278$ MPa. The material is assumed to be perfectly elastic–plastic without a strain-hardening effect.

In the case of considering the strain rate, the Cowper–Symonds model has proven to be applicable for steel structures by experiment results [28,29], as seen in the following Equation (1).

$$\frac{\sigma_d}{\sigma_s} = 1 + \left(\frac{\dot{\epsilon}}{D} \right)^{1/q} \tag{1}$$

where σ_d denotes the dynamic stress, σ_s denotes the static stress; D and q are the material parameters. $D = 40.4$, $q = 5$ is used for the mild steel in the present study.

3.3. Meshing Density

Generally, a rectangular element with a length–width aspect ratio close to 1.0 was chosen for the non-linear FE analysis. Under the static loading condition, the meshing density of 6~10 elements in one plate width is enough to obtain a reasonable calculation

result. Figure 4 shows that the calculation results of the ultimate bending moment of the box girder with 10 elements along one plate width is a little lower than that with four or six elements. The initial imperfection of two half-waves with an amplitude of 0.9 mm is applied in the analysis. When the element number exceeds 10, the calculation results of the ultimate bending moment show a stable value.

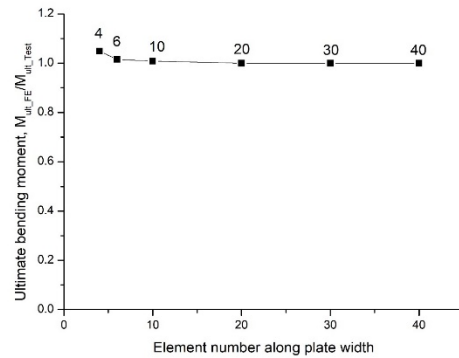


Figure 4. Ultimate bending moment of box girder with various meshing density under static load (initial imperfection assumed as 2 half-wave with the amplitude 0.9 mm).

In the dynamic explicit calculation method, the stability limit of the calculation has a relationship with the characteristic element length, i.e., the minimum element length. The shorter the element length is, the shorter the calculation time of the increase step. In order to control the calculation time of the structural response, it had better not use an overfine mesh density. In the following analysis, a mesh density with 20 elements along one plate width was used, as shown in Figure 5. The meshing size is about 9 mm for the FE analysis. There are 20 elements along the plating width, 60 elements along the plating length, six elements along the stiffener web height and eight elements along the frame web width.

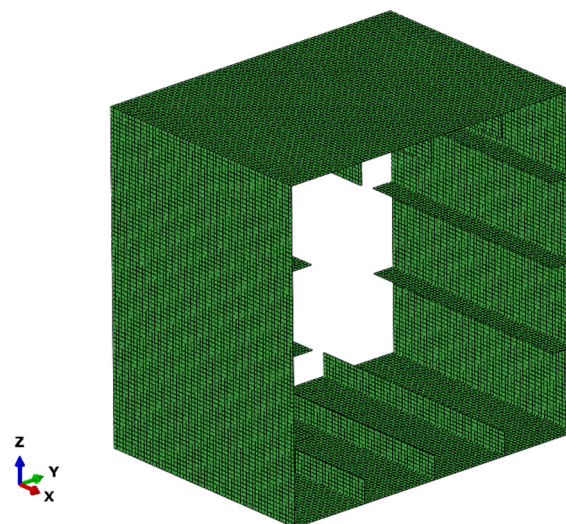


Figure 5. Mesh density of one span in the middle.

3.4. Initial Imperfections

For the simply supported plate, the buckling half-wave number m in plate length direction can be estimated by using the following Equation (2):

$$\frac{a}{b} \leq \sqrt{m(m+1)} \tag{2}$$

where a is the plate length, b is the plate width and m is the buckling half-wave number.

For the box girder in this paper, $a = 540$ mm and $b = 180$ mm; therefore, the buckling half-wave number is $m = 3$. In order to trigger the failure mode, the initial imperfection can

be assumed as the buckling mode with three half-waves in the plate length direction and one half-wave buckling mode in the plate width. This paper also considers the effect of initial imperfection with two half-waves and four half-waves in the plate length direction, as shown in Figure 6. The initial imperfection is applied to the compressed upper panel of a box girder under the bending moment.

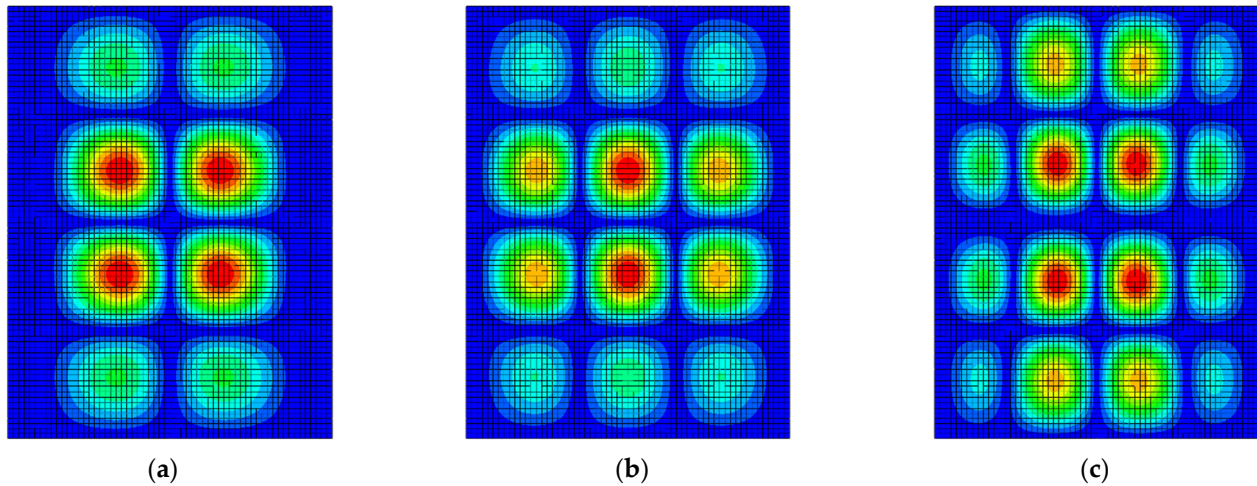


Figure 6. Initial imperfections with different half-waves along plate length and one half-wave along plate width between longitudinal stiffeners (a) 2 half-waves, (b) 3 half-waves, (c) 4 half-waves.

The effect of various imperfection types and various imperfection amplitudes on the ultimate bending moment of a box girder is shown in Figure 7. When the amplitude of the initial imperfection is the same, the imperfection with three half-waves gives the lowest estimation of the ultimate bending moment. For the same type of imperfection, the ultimate bending moment almost shows a linear reduction with the increase in the imperfection amplitude.

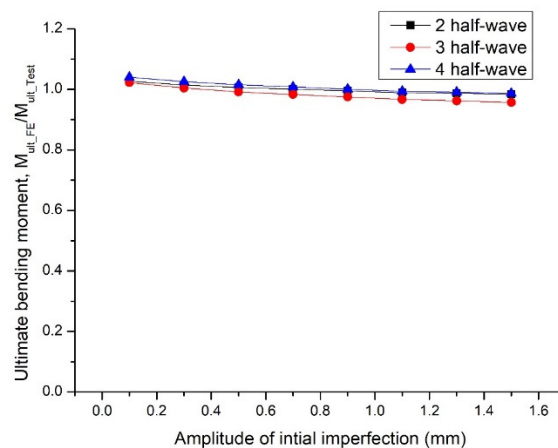


Figure 7. Ultimate bending moment of box girder with various imperfection under static load.

In the following analysis, the initial imperfection type is assumed to be in the three-half-wave buckling mode in the plate length direction, and the imperfection amplitude is assumed to be $b/200 = 180/200 = 0.9$ mm. This assumption is often adopted in ship rule research in the IACS (2014) classification societies.

The comparison of non-linear FE results and experiment results is shown in Figure 7. Through the use of FE analysis, the ultimate bending moment of the box girder is $M_{ult,s} = 5.74 \times 10^8$ Nmm, and the displacement of the mid-span at the limit state is $W_{ult,s} = 14.6$ mm. The value of the ultimate bending moment and displacement at the limit state by FE is almost close to the experiment result under the static condition. However, the load and displacement

curves of the FE results and experiment results are not perfectly consistent. Perhaps, there are some differences between the actual imperfection in the experiment and the assumed imperfection in the FE analysis.

Under the static load conditions, the Riks method is used to carry out non-linear ultimate strength analysis. Riks' method is based on the load increment controlled by a scalar parameter of the arc length. In the following dynamic analysis, the Riks method should be replaced by the Dynamic Explicit solver, which is based on the central difference algorithm and easily obtains the convergent solution.

4. Dynamic Ultimate Strength of Box Girder under Bending Moment

The validated non-linear FE analysis method, including the boundary conditions, material properties, meshing density and initial imperfection, are extended to calculate the dynamic response of the box girder. Compared with the static load conditions, several differences should be specially considered in dynamic analysis in the time domain, including mass density, strain rate and the load change over time.

Based on the box girder of MST-3 in the Nishihara experiment, six box girder models are designed with the same cross-section scantlings and span length, as listed in Table 2. Compared with each model, the model length, plate thickness and material density have a slight difference in order to study the relevant influence factors.

Table 2. Box girder models for dynamic ultimate strength analysis.

Model	Model Length	Plate Thickness	Yielding Strength	Material Density	Static Ultimate Moment	Ultimate Displacement at Mid-Span	Natural Vibration Period
	$L, \text{ mm}$	$t_p, \text{ mm}$	$R_{eH}, \text{ MPa}$	$\rho, \text{ t/mm}^3$	$M_{ult_s}, \text{ Nmm}$	$W_{ult_s}, \text{ mm}$	$T_0, \text{ s}$
M1	3780	3.05	278	7.89×10^{-9}	5.71×10^8	6.1	0.011
M2	5940	3.05	278	7.89×10^{-9}	5.74×10^8	14.6	0.025
M3	5940	4.0	278	7.89×10^{-9}	9.46×10^8	15.3	0.023
M4	5940	5.0	278	7.89×10^{-9}	1.29×10^9	17.4	0.022
M5	5940	3.05	278	1.58×10^{-8}	5.74×10^8	14.6	0.029
M6	5940	3.05	278	2.37×10^{-8}	5.74×10^8	14.6	0.034

Note: T_0 corresponds to the fundamental natural vibration mode of the box girder models.

The ultimate bending moment under the static conditions is also listed in Table 2. Models M1, M2, M5 and M6 almost have the same ultimate bending moment. That is to say, model length and material density have little effect on the calculation results under static conditions. However, the natural vibration periods of the six models are different. Therefore, the dynamic response of these models may also be different under the same dynamic loads.

4.1. Dynamic Bending Moment of Box Girder

The dynamic loads of $F_1 = F_2$ are applied to the upper edge of the bulkhead (BHD), as shown in Figure 3. Based on the water basin test of the girder under whipping loads [17] and the falling hammer test of the girder under impact loads [19], the load time history in the action period can be simplified as a half-sine shape with time. Therefore, the dynamic loads are assumed as a half-sine shape in this paper. The mid-ship bending moment can be evaluated according to the theory of simple support girder [30]. The external applied bending moment by the applied load at the mid-span of the box girder can be calculated as following Equation (3):

$$M(t) = \begin{cases} F_1 \cdot L_1 \cdot \sin\left(\frac{2\pi t}{T_d}\right) & \text{if } 0 \leq t \leq T_d \\ 0 & \text{if } t > T_d \end{cases} \quad (3)$$

where t is the response calculation time, T_d is the load duration time, T_e is the excitation period $T_e = 2 * T_d$, F_1 is the applied dynamic load amplitude and L_1 the distance between the applied load position and the pinned point.

As the load duration time T_d is changed, the excitation period T_e will be updated, leading to a specific ratio to the natural vibration period T_0 of the box girder.

The external applied dynamic bending moment will be withstood by the box girder deformation and inertia forces. Owing to the box girder deformation, the internal bending moment at each cross-section can be derived. Under the static load conditions, the internal bending moment is equal to the external applied bending moment at the same cross-section. However, under dynamic load conditions, the internal bending moment may be smaller than the external applied bending moment due to the inertia effect when the dynamic duration time is very short.

In the early dynamic stage, the internal moment at the mid-span is large and the upper stiffened panel is in compression, which is similar as the sagging moment. After the peak of the dynamic load, the bending moment at the mid-span reduces progressively, and then the opposite bending deformation of the box girder may be activated, leading to the opposite value of the internal bending moment, which is similar to the hogging moment. Therefore, the sagging–hogging internal moment will occur and alternately change over time, as shown in Figure 8. When the applied external bending moment reduces to 0 at a response calculation time of $t > T_d$ in Equation (3), the internal bending moment will still occur due to the girder vibration deformation.

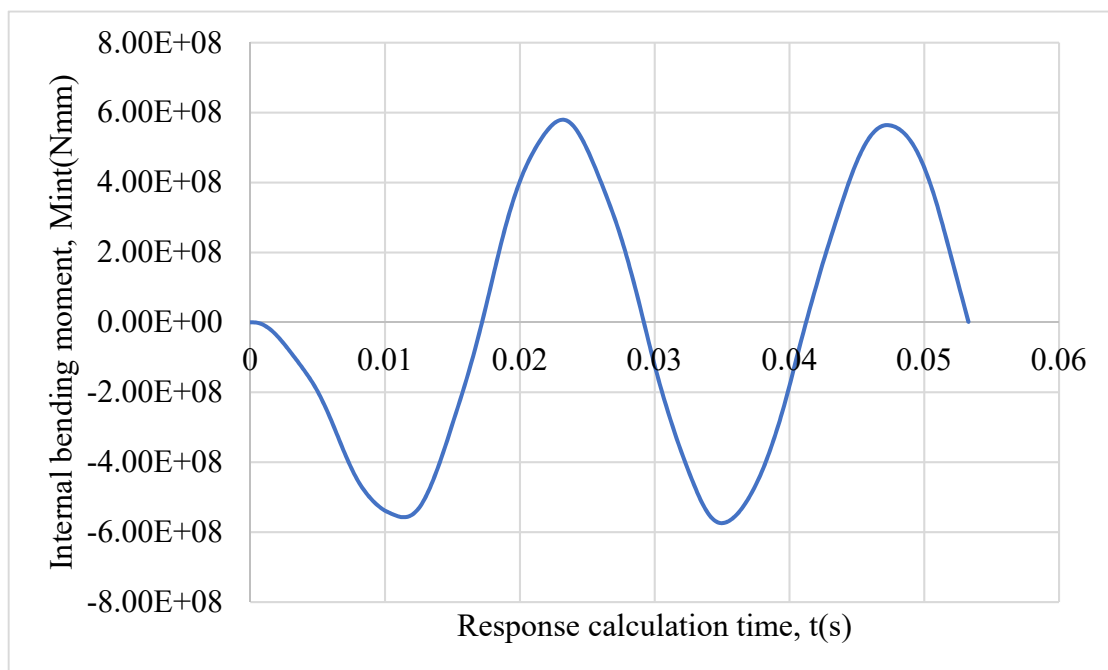


Figure 8. Internal bending moment of mid-section when the applied dynamic bending moment $M_d = 1.0M_{ult,s}$ and the dynamic load duration time $T_d = 0.9 T_0$.

The external applied bending moment is taken as the capacity index of the box girder in this paper, which is convenient for evaluating the external dynamic load condition.

4.2. Dynamic Response of Box Girder under Bending Moment

For the M2 box girder, a series of different amplitudes of dynamic bending moment M_d are applied as a sinusoidal shape, including $1.0M_{ult,s}$, $2.0M_{ult,s}$, $3.0M_{ult,s}$ and $4.0M_{ult,s}$. The load duration time is taken as $T_d = 0.005$ s, which is close to the drop hammer impact time in the experiment on the box girder [31]. The load duration time T_d is about 0.2 times

that of the natural vibration period T_0 of the M2 box girder. Therefore, the box girder will show an apparent dynamic response under this load assumption.

The response calculation time includes the load duration time and two vibration periods, with no external applied loads to evaluate the free vibration response after the dynamic load action stage. The response calculation time is divided by half of the natural vibration period of T_0 .

The vertical displacement W_d at the mid-span is derived by averaging all of the node displacements of the cross-section and then divided by the limit displacement $W_{ult,s}$ of the same cross-section under a static bending moment. This treatment can yield a dimensionless index of vertical displacement and is convenient for comparing the dynamic and static responses.

The vertical displacement responses at the mid-span as the response calculation time for the M2 box girder are shown in Figure 9. For $M_d = 1.0 M_{ult,s}$, the box girder shows an elastic response, and the hogging (bending upwards)–sagging (bending downwards) vibration deformation amplitude is almost symmetrical. For $M_d = 2.0 M_{ult,s}$, the sagging deformation is larger than the hogging. For $M_d = 3.0 M_{ult,s}$, the vibration mode has been changed, and the value of dynamic deformation is always negative due to the large plastic deformation after dynamic load. For $M_d = 4.0 M_{ult,s}$, the vibration period T_1 (between two neighboring peaks in the free vibration stage) after dynamic load action exceeds the natural vibration period T_0 due to large failure areas induced by local buckling and plastic deformation.

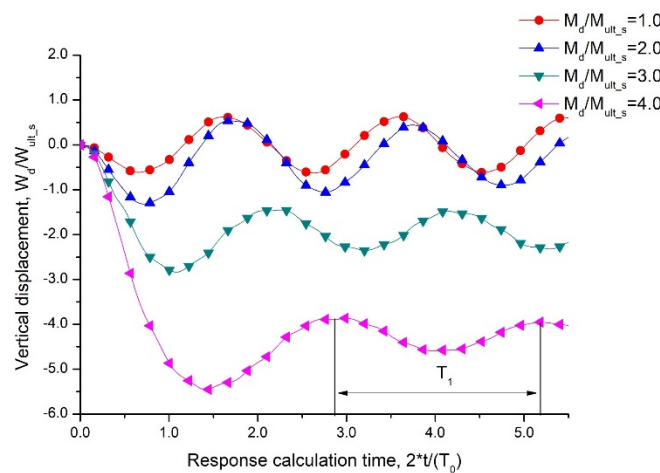


Figure 9. Vertical displacement response at mid-span as the response calculation time for box girder M2 with load duration time $T_d = 0.005$ s.

The Mises stress and deformation distribution at the time of the maximum vertical displacement for the mid-span of the M2 box girder are shown in Figure 8. Only in the load case of $M_d = 1.0M_{ult,s}$ was the stress lower than the static yield strength. The maximum value of the Mises stress for the load case of $M_d = 4.0M_{ult,s}$ is about 400 MPa, which is higher than the static yield strength. Based on Equation (1), the strain rate for the box girder is about 1/s~10/s, which shows the dynamic characteristics.

The deformed shape is also shown in Figure 10. There are three half-wave buckling modes in the upper panel of the box girder. The difference between load case $M_d = 2.0M_{ult,s}$ and $M_d = 3.0M_{ult,s}$ is evident. For load case $M_d = 2.0M_{ult,s}$, there is one cross-section with apparent deformation. However, for load case $M_d = 3.0M_{ult,s}$, there are three cross-sections with apparent deformation at the same time, which is different from the limit deformation under static load conditions.

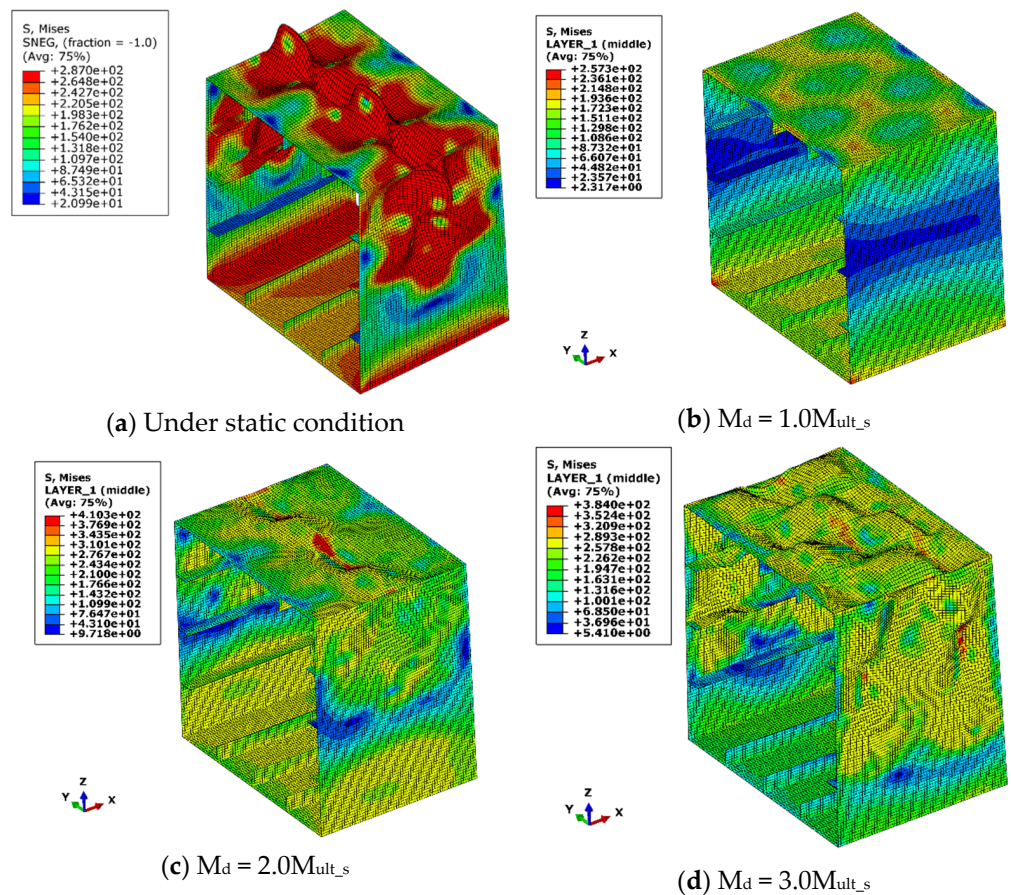


Figure 10. Mises stress and deformation distribution at the time of maximum vertical displacement for the mid-span of box girder M2 with load duration time $T_d = 0.005$ s.

4.3. Evaluation Criterion of Dynamic Ultimate Strength for Box Girder

Based on the relationship between dynamic loads and structural dynamic responses, the dynamic ultimate strength evaluation is meaningful in guiding structure design and safety evaluation. However, the bending moment and vertical displacement curve under dynamic loads will not show an extreme value or sudden change because of the stable post-buckling path for the box girder. A reasonable evaluation criterion for dynamic ultimate strength is needed.

The B-R criterion [21] was proposed to evaluate the dynamic buckling of a plate. For box girders with stiffened panels, plate buckling can be regarded as one kind of local buckling. The box girder will have a stable post-buckling path, so the load–displacement will not present a severely rapid increase as the plate buckling. The B-R criterion should be revised based on the response characteristics of the box girder under a dynamic bending moment.

The internal bending moment can be derived based on the bending stresses and their locations in the cross-section of a hull girder. The curve of the internal bending moment and vertical displacement at the mid-span section is shown in Figure 11. The applied bending moment ratio ($M_d/M_{ult,s}$) is also plotted in Figure 11 using data labels.

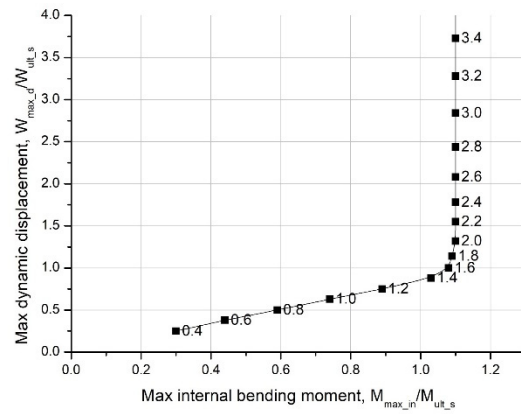


Figure 11. Internal bending moment and vertical displacement for mid-span box girder M2 at load duration time $T_d = 0.005$ s (Data label denotes M_d/M_{ult_s}).

When the applied bending moment ratio is small, i.e., $M_d/M_{ult_s} < 1.4$, the vertical displacement shows an almost linear trend of increase as an increase in the bending moment. When the applied bending moment ratio is $1.4 > M_d/M_{ult_s} < 2.0$, the curve of the internal bending moment and vertical displacement becomes non-linear, which denotes some local failure induced by buckling and yielding occurring on the box girder. When the applied bending moment ratio is $M_d/M_{ult_s} \geq 2.0$, the internal bending moment at the mid-span of the box girder reaches its peak value. The internal bending moment will not increase as the applied bending moment, but the max displacement at the mid-span shows a rapid increase. It is an obvious signal that the box girder has reached its dynamic limit state. Therefore, the evaluation criterion of the dynamic limit state of the box girder is the curve of the internal bending moment, and vertical displacement reaches the extreme point.

For the load duration time of $T_d = 0.01$ s and $T_d = 0.016$ s, the curves of the internal bending moment and vertical displacement are shown in Figures 12 and 13. The same trend of the extreme point can be found. The proposed evaluation criterion of the dynamic limit state can be applicable to more load cases.

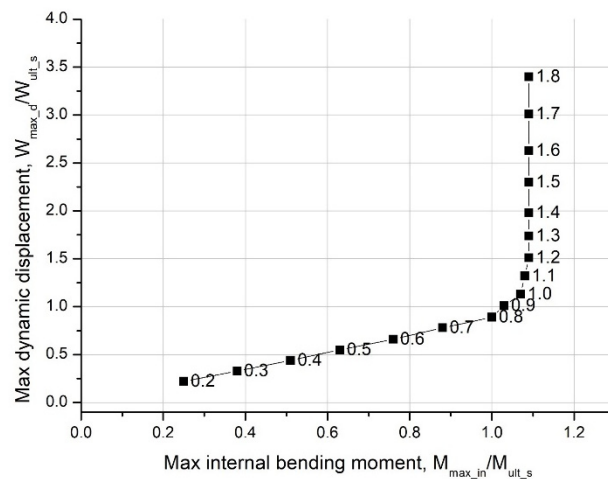


Figure 12. Internal bending moment and vertical displacement for mid-span box girder M2 at load duration time $T_d = 0.01$ s (Data label denotes M_d/M_{ult_s}).

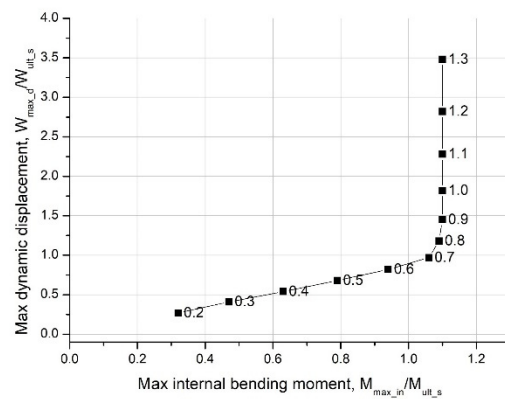


Figure 13. Internal bending moment and vertical displacement for mid-span box girder M2 at load duration time $T_d = 0.016$ s (Data label denotes $M_d/M_{ult,s}$).

The applied bending moment at the dynamic limit state for the load duration time $T_d = 0.005$ s, $T_d = 0.01$ s and $T_d = 0.016$ s are summarized in Table 3. As the load duration time increases, the dynamic effect for the box girder is not very obvious, and the applied bending moment at the dynamic limit state will approach the ultimate bending strength at the static limit state.

Table 3. Dynamic ultimate strength of the box girder.

Model	Load Duration Time		Applied Bending Moment at Dynamic Limit State
	T_d, s	$2T_d/T_0$	$M_{ult,d}/M_{ult,s}$
M2	$T_d = 0.005$ s	0.4	2.0
M2	$T_d = 0.01$ s	0.8	1.2
M2	$T_d = 0.016$ s	1.3	1.0

5. Influence Factors on Dynamic Ultimate Strength of Box Girder

For box girders, there are several influencing factors on dynamic ultimate strength. This paper tries to study these four factors, including model length, plate thickness, material density and load duration time.

5.1. Effect of Model Length

Each span of the box girder is strengthened by transverse frames or bulkheads at two ends. The model length is set as the product of span number and span length. The box girder M1 has seven spans and a 3780 mm model length. The box girder M2 has 11 spans and a 5940 mm model length. The ratio of model length L and span length S appears to be a non-dimensional parameter. Both models have the same cross-section scantlings and span length. These models are assumed to have the initial imperfection of the three half-wave, with an amplitude of 0.9 mm of mid-span.

As we all know, the span number in the analysis model has little effect on the static ultimate bending moment when the span number is larger [32] and the span length is kept unchanged. Therefore, two- or three-span FE models are often used in static ultimate strength analysis for box girders.

Under dynamic conditions, the curve of the internal bending moment and vertical displacement at the mid-span section for the M1 box girder with load duration times of $T_d = 0.005$ s and $T_d = 0.016$ s are shown in Figures 14 and 15. Based on the proposed evaluation criterion, the applied bending moment ratio $M_{ult,d}/M_{ult,s}$ at the dynamic limit state is listed in Table 4. For the load duration time $T_d = 0.005$ s, the dynamic ultimate moment of box girder M1 (length ratio $L/S = 7$) is lower than that of box girder M2 (length ratio $L/S = 11$). However, for a load duration time of $T_d = 0.016$ s, there is no obvious

dynamic effect, and the ultimate moment of box girder M1 and M2 is the same. It can be concluded that the model length ratio has a great influence on the dynamic ultimate moment at shorter load duration times. The longer model shows a larger dynamic carrying capacity. There are two reasons to explain this phenomenon. (1) The longer model has a greater inertia load along the model length direction, which needs a greater applied load to cause structural failure; (2) the longer model has a longer first vibration period, which shows more obvious dynamic effects for the load with duration time less than the first vibration period. It is recommended that a full-length model should be used in dynamic strength analysis instead of the simplified one-span model.

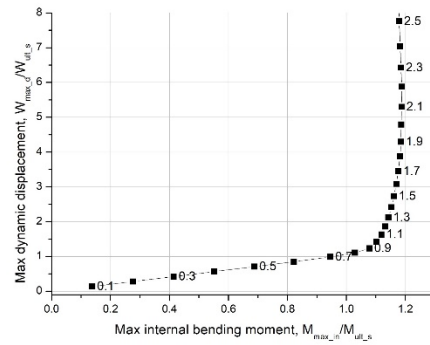


Figure 14. Internal bending moment and vertical displacement for mid-span box girder M1 at load duration time $T_d = 0.005$ s (Data label denotes $M_d/M_{ult,s}$).

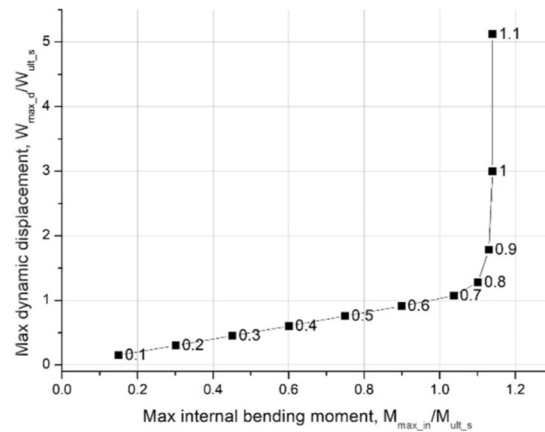


Figure 15. Internal bending moment and vertical displacement for mid-span box girder M1 at load duration time $T_d = 0.016$ s (Data label denotes $M_d/M_{ult,s}$).

Table 4. Comparison of dynamic ultimate moment for box girder with various length.

Model	Model Length	Length Ratio	Load Duration Time	Applied Bending Moment at Dynamic Limit State
	$L, \text{ mm}$	L/S	$T_d, \text{ s}$	$M_{ult,d}/M_{ult,s}$
M1	3780	7	0.005	1.7
M2	5940	11	0.005	2.0
M1	3780	7	0.016	1.0
M2	5940	11	0.016	1.0

5.2. Effect of Plate Thickness

The plate thickness is the critical parameter of structure stiffness. Three kinds of plate thickness t_p are set on the plate and stiffener web of the box girder. For box girders M2,

M3 and M4, the plate thicknesses are $t_p = 3.05$, $t_p = 4.0$ and $t_p = 5.0$, respectively. The plate slenderness ratio β can be considered a non-dimensional parameter. As the plate thickness increases, the natural vibration period T_0 has a little decrease, as shown in Table 2.

The curve of the internal bending moment and vertical displacement at the mid-span section for box girder M3 and M4 with a load duration time of $t_d = 0.005$ s are shown in Figures 16 and 17. The comparison of dynamic ultimate moment for box girder with a plate slenderness ratio of β is listed in Table 5. As the plate slenderness ratio of β changes, the applied bending moment ratio at the dynamic limit state is almost unchanged. That is to say, the dynamic effect for these girders will show a similar trend for the dynamic load with the same load duration time. It should be noted that the actual dynamic bending capacity of models M3 and M4 is higher than that of model M2 due to the increased static ultimate strength $M_{ult,s}$, as shown in Table 2.

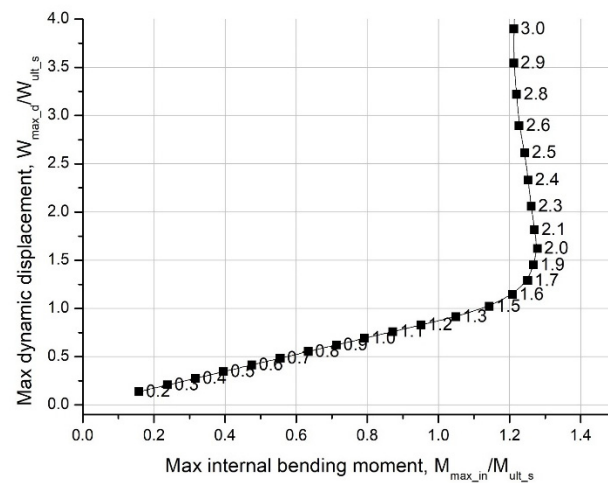


Figure 16. Internal bending moment and vertical displacement for mid-span box girder M3 at load duration time $T_d = 0.005$ s (Data label denotes $M_d/M_{ult,s}$).

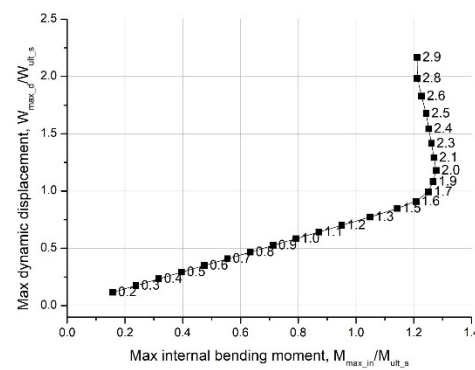


Figure 17. Internal bending moment and vertical displacement for mid-span box girder M4 at load duration time $T_d = 0.005$ s (Data label denotes $M_d/M_{ult,s}$).

Table 5. Comparison of dynamic ultimate moment for box girder with various plate thickness.

Model	Plate Thickness	Plate Slenderness Ratio	Load Duration Time	Applied Bending Moment at Dynamic Limit State
	t_p , mm	β	T_d , s	$M_{ult,d}/M_{ult,s}$
M2	3.05	2.2	0.005	2.0
M3	4	1.7	0.005	2.0
M4	5	1.3	0.005	2.0

5.3. Effect of Material Density

In actual ship structures, the box girder should withstand its structural weight and non-structure weight, including liquid/dry cargo, ballast water and fuel oil and so on. For dynamic response analysis, the changes of the mass point and density are often used to simulate various mass distribution conditions. The change in density is used in this paper to study the effect of mass distribution on dynamic ultimate moment.

In order to model the supplementary onboard distributed masses, two other kinds of equivalent material density are assumed in models M5 and M6, as shown in Table 2. The box girders of M5 and M6 are set as two times and three times of material density of M2, respectively. Although M2, M5 and M6 have the same cross-section scantlings, the box girders of M5 and M6 have longer natural vibration periods than that of M2, as shown in Table 2.

The bending moment and vertical displacement curve of the applied bending moment and vertical displacement at the mid-span section for box girders M5 and M6 with a load duration time of $t_d = 0.005$ s are shown in Figures 18 and 19. The relative density between the analysis model and the based model (M2) is defined. A comparison of the dynamic ultimate moment of the box girders with various densities is listed in Table 6. The larger the model's relative density, the higher the dynamic ultimate moment ratio. Material density should be assumed to be a critical factor in dynamic ultimate strength analysis.

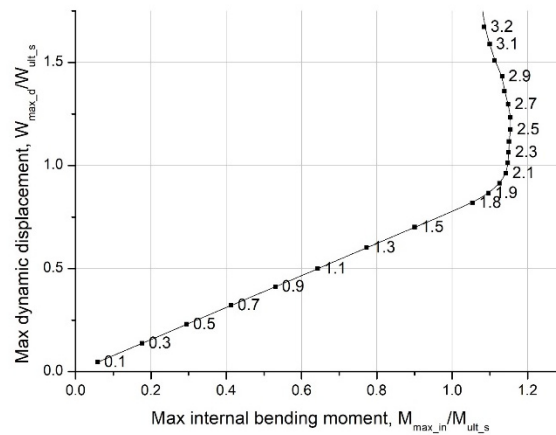


Figure 18. Internal bending moment and vertical displacement for mid-span box girder M5 at load duration time $T_d = 0.005$ s (Data label denotes $M_d/M_{ult,s}$).

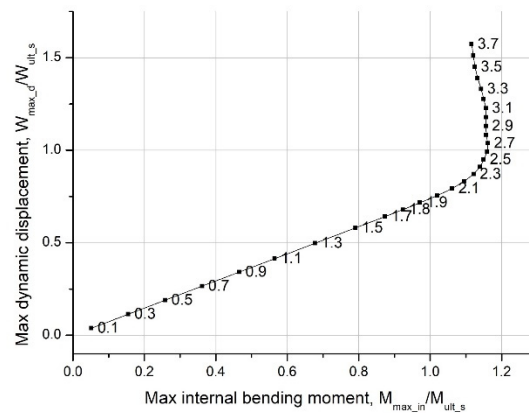


Figure 19. Internal bending moment and vertical displacement for mid-span box girder M6 at load duration time $T_d = 0.005$ s (Data label denotes $M_d/M_{ult,s}$).

Table 6. Comparison of dynamic ultimate moment of box girder with various density.

Model	Material Density	Relative Density	Load Duration Time	Applied Bending Moment at Dynamic Limit State
	$\rho, t/mm^3$	ρ/ρ_{M2}	T_d, s	M_{ult_d}/M_{ult_s}
M2	7.89×10^{-9}	1.0	0.005	2.0
M5	1.58×10^{-8}	2.0	0.005	2.5
M6	2.37×10^{-8}	3.0	0.005	2.7

5.4. Effect of the Excitation Period

This paper assumes that the dynamic load has a half-sine shape and the start time as the beginning of the response calculation. The load duration time T_d is set from 0.004 to 0.025 s, which covers the scope of drop hammer impact on stiffened panel of steel and also the interval of box girder vibration period. The excitation period is two times that of the duration time, i.e., $T_e = 2 \times T_d$. The ratio T_e/T_0 between the excitation period and the natural vibration period can be considered a non-dimensional parameter.

The comparison of dynamic ultimate moment ratio of box girder with various load excitation period ratios T_e/T_0 is listed in Table 7. The shorter the load duration time ratio, the larger the dynamic ultimate moment. The dynamic ultimate moment ratio M_{ult_d}/M_{ult_s} is within the scope from 1.0 to 2.5 for the load duration time ratio of larger than 0.3. When the load excitation period ratio T_e/T_0 is larger than 1.3, the dynamic effect is not very obvious for box girder under bending moment.

Table 7. Comparison of applied ultimate moment ratio at dynamic limit state of box girder (Model M2) with various load duration time.

Load Excitation Period	Load Excitation Period Ratio	Applied Bending Moment at Dynamic Limit State
$T_e = 2 \times T_d, s$	T_e/T_0	M_{ult_d}/M_{ult_s}
0.008	0.3	2.3
0.010	0.4	2.0
0.016	0.7	1.4
0.020	0.8	1.2
0.026	1.1	1.1
0.032	1.3	1
0.036	1.5	1
0.050	2.0	1

Based on the FE results evaluated by proposed criterion, the relationship of dynamic ultimate moment ratio M_{ult_d}/M_{ult_s} and the load excitation period ratio T_e/T_0 is plotted in Figure 20. When the load duration time ratio increases, the dynamic ultimate moment ratio gradually decreases.

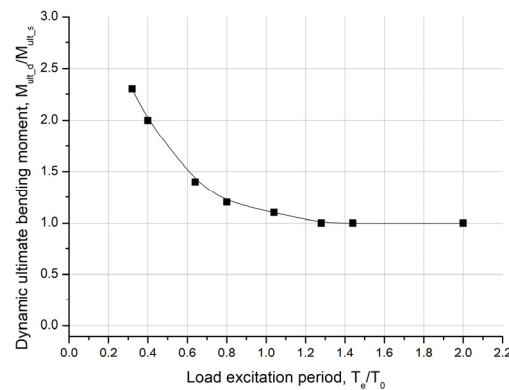


Figure 20. Effect of load excitation period on dynamic ultimate moment of box girder M2.

6. Conclusions

The main conclusions can be drawn as follows:

(1) Under larger applied dynamic moments, the box girder vibration period will be increased due to local buckling and plastic deformation. In the dynamic loading case, there are more than one cross-section with apparent deformation at the same time, which is different from only cross-section failure in the static loading case.

(2) An evaluation criterion of dynamic limit state for box girder under bending is proposed in this paper based on the curve of internal bending moment and vertical displacement, which can give reasonable prediction of dynamic ultimate strength.

(3) The model length has a great influence on the applied dynamic ultimate moment at shorter load duration times. The longer model needs a larger dynamic moment to reach the limit state. The full-length model is recommended to use in dynamic analysis.

(4) The larger the relative density of the box girder, the higher its dynamic ultimate moment ratio $M_{ult,d}/M_{ult,s}$ due to the inertia effect. The material density should be considered a critical factor in dynamic ultimate strength analysis.

(5) When the load excitation period ratio T_e/T_0 is larger than 1.3, the dynamic effect is not very obvious for box girder bending, and the load action will be close to the quasistatic condition. For the load excitation period ratio T_e/T_0 with the scope of 0.3 and 1.3, the dynamic ultimate moment ratio $M_{ult,d}/M_{ult,s}$ is within the scope of 2.5 to 1.0.

Author Contributions: Writing-original, G.-J.S.; Study design, D.-Y.W.; Formal analysis, F.-H.W.; Validation, S.-J.C. All authors have read and agreed to the published version of the manuscript.

Funding: This research was funded by National Natural Science Foundation of China (Grant No.51809168, Grant No.51979163, and Grant No. U2241266).

Data Availability Statement: Data will be made available on request.

Conflicts of Interest: The authors declare that they have no known competing financial interests or personal relationships that could have appeared to influence the work reported in this paper.

Nomenclature

$M_{ult,s}$	Bending moment at the limit state of box girder under static condition
$M_{ult,d}$	Bending moment at the limit state of box girder under dynamic condition
$M_{max,in}$	Max internal bending moment of box girder
M_d	Amplitude of applied dynamic bending moment of box girder
$W_{ult,s}$	Vertical displacement along Z direction of box girder mid-span section at the limit state under static condition
W_d	Vertical displacement along Z direction of box girder mid-span section during dynamic load

W_{\max_d}	Maximum vertical displacement along Z direction of box girder mid-span section in the whole response calculation time (including dynamic load duration time and free vibration time after the dynamic load)
W_{p_d}	Permanent displacement after dynamic loading along Z direction of box girder mid-span section after dynamic load
t	Response calculation time
T_0	Natural vibration period of box girder
T_1	Vibration period (between two neighboring peaks in free vibration stage) of box girder after dynamic load action
T_d	Dynamic load duration time
L	Analysis model length
S	Span length between neighboring transverse frame
β	Plate slenderness ratio $\beta = b/t\sqrt{\sigma_Y/E}$
X axis	Along the box girder length direction
Y axis	Along the box girder width direction
Z axis	Along the box girder height direction

References

- Al-Rifaie, A.; Guan, Z.W.; Jones, S.W.; Wang, Q. Lateral impact response of end-plate beam-column connections. *Eng. Struct.* **2017**, *151*, 221–234. [CrossRef]
- Budiansky, B.; Roth, R. Axisymmetric buckling of clamped shallow spherical shells. *NASA TND* **1962**, *1510*, 597–606.
- CLCSS. Final Report of Committee on Large Container Ship Safety. Japan Committee on Large Ship Safety. 2015. Available online: <https://www.mlit.go.jp/common/001081297.pdf> (accessed on 30 January 2023).
- Derbanne, Q.; De Lauzon, J.; Bigot, F.; Malenica, S. Investigations of the dynamic ultimate strength of a ship's hull girder during whipping. In Proceedings of the PRADS, Copenhagen, Denmark, 4–8 September 2016.
- DNV-GL. Classification Notes No.30.12: Fatigue and Ultimate Strength Assessment of Container Ships Including Whipping and Springing. 2015. Available online: https://global.ihs.com/doc_detail.cfm?document_name=DNVGL%2DCG%2D0153&item_s_key=00663928 (accessed on 30 January 2023).
- Duarte, I.; Vesenjak, M.; Krstulović-Opara, L. Dynamic and quasi-static bending behaviour of thin-walled aluminium tubes filled with aluminium foam. *Compos. Struct.* **2014**, *109*, 48–56. [CrossRef]
- Hansen, A.M. Strength of midship sections. *Mar. Struct.* **1996**, *9*, 471–494. [CrossRef]
- Hu, K.; Yang, P.; Xia, T.; Peng, Z. Residual ultimate strength of large opening box girder with crack damage under torsion and bending loads. *Ocean Eng.* **2018**, *162*, 274–289. [CrossRef]
- Huang, Z.; Zhang, X. Three-point bending collapse of thin-walled rectangular beams. *Int. J. Mech. Sci.* **2018**, *144*, 461–479. [CrossRef]
- Iijima, K.; Suzuki, Y.; Fujikubo, M. Scaled model tests for the post-ultimate strength collapse behaviour of a ship's hull girder under whipping loads. *Ships Offshore Struct.* **2015**, *10*, 31–38. [CrossRef]
- Jagite, G.; Bigot, F.; Derbanne, Q.; Malenica, Š.; Le Sourne, H.; de Lauzon, J.; Cartraud, P. Numerical investigation on dynamic ultimate strength of stiffened panels considering real loading scenarios. *Ships Offshore Struct.* **2019**, *14*, 374–386. [CrossRef]
- Jagite, G.; Bigot, F.; Malenica, S.; Derbanne, Q.; Le Sourne, H.; Cartraud, P. Dynamic ultimate strength of a ultra-large container ship subjected to realistic loading scenarios. *Mar. Struct.* **2022**, *84*, 103197. [CrossRef]
- Jagite, G.; le Sourne, H.; Cartraud, P.; Bigot, F.; Derbanne, Q.; Malenica, Š. Dynamic ultimate strength of a container ship under sagging condition. In *International Conference on Offshore Mechanics and Arctic Engineering*; American Society of Mechanical Engineers: New York, NY, USA, 2020.
- Jagite, G.; Le Sourne, H.; Cartraud, P.; Bigot, F.; Derbanne, Q.; Malenica, Š. Examination of the dynamic effects on the hull girder ultimate strength of ultra large container ships. *Trends Anal. Des. Mar. Struct.* **2019**, 137–148.
- Kaewunruen, S.; Remennikov, A.M. Progressive failure of prestressed concrete sleepers under multiple high-intensity impact loads. *Eng. Struct.* **2009**, *31*, 2460–2473. [CrossRef]
- Li, D.; Feng, L.; Huang, D.; Shi, H.; Wang, S. Residual ultimate strength of stiffened box girder with coupled damage of pitting corrosion and a crack under vertical bending moment. *Ocean Eng.* **2021**, *235*, 109341. [CrossRef]
- Lim, H.K.; Lee, J. On the structural behavior of ship's shell structures due to impact loading. *Int. J. Nav. Archit. Ocean. Eng.* **2018**, *10*, 103–118. [CrossRef]
- Liu, W.; Suzuki, K.; Shibamura, K.; Pei, Z. Nonlinear Dynamic Response and Strength Evaluation of a Containership in Extreme Waves Based on Hydroelastoplasticity Method. In Proceedings of the Twenty-fourth International Ocean and Polar Engineering Conference, Busan, Korea, 15–20 June 2014.
- Liu, X.; Jiang, D.; Liufu, K.; Fu, J.; Liu, Q.; Li, Q. Numerical investigation into impact responses of an offshore wind turbine jacket foundation subjected to ship collision. *Ocean. Eng.* **2022**, *248*, 110825. [CrossRef]
- MAIB. Report on the Investigation of the Structural Failure of MSC Napoli; Marine Accident Investigation Branch: London, UK, 2008.

21. Nassirnia, M.; Heidarpour, A.; Zhao, X.-L.; Wang, R.; Li, W.; Han, L.-H. Hybrid corrugated members subjected to impact loading: Experimental and numerical investigation. *Int. J. Impact Eng.* **2018**, *122*, 395–406. [[CrossRef](#)]
22. Nishihara, S. Ultimate longitudinal strength of mid-ship cross section. *Nav. Archit. Ocean. Eng.* **1984**, *22*, 200–214.
23. Paik, J.K. *Ultimate Limit State Analysis and Design of Plated Structures*, 2nd ed; Wiley: New York, NY, USA, 2018.
24. Pham, T.M.; Hao, H. Plastic hinges and inertia forces in RC beams under impact loads. *Int. J. Impact Eng.* **2017**, *103*, 1–11. [[CrossRef](#)]
25. Sun, G.; Deng, M.; Zheng, G.; Li, Q. Design for cost performance of crashworthy structures made of high strength steel. *Thin-Walled Struct.* **2018**, *138*, 458–472. [[CrossRef](#)]
26. Volmir, S.A. *Nonlinear Dynamics of Plates and Shells*, Science, Moscow, 1972. Available online: <https://trid.trb.org/view/17770> (accessed on 30 January 2023).
27. Wei, J.; Li, J.; Wu, C.; Liu, Z.-X.; Fang, J. Impact resistance of ultra-high performance concrete strengthened reinforced concrete beams. *Int. J. Impact Eng.* **2021**, *158*, 104023. [[CrossRef](#)]
28. Xu, M.C.; Song, Z.J.; Pan, J. Study on influence of nonlinear finite element method models on ultimate bending moment for hull girder. *Thin-Walled Struct.* **2017**, *119*, 282–295. [[CrossRef](#)]
29. Xu, M.C.; Song, Z.J.; Pan, J. Study on the similarity methods for the assessment of ultimate strength of stiffened panels under axial load based on tests and numerical simulations. *Ocean Eng.* **2020**, *219*, 108294. [[CrossRef](#)]
30. Yamada, Y. Dynamic Collapse Mechanism of Global Hull Girder of Container Ships Subjected to Hogging Moment. *J. Offshore Mech. Arct. Eng.* **2019**, *141*, 1–15. [[CrossRef](#)]
31. Yang, B.; Wang, D.-Y. Dynamic Ultimate Hull Girder Strength Analysis on a Container Ship under Impact Bending Moments. *Int. J. Offshore Polar Eng.* **2018**, *28*, 105–111. [[CrossRef](#)]
32. Zanuy, C.; Ulzurrun, G.S.; Curbach, M. Experimental determination of sectional forces in impact tests: Application to composite RC-HPFRCC beams. *Eng. Struct.* **2022**, *256*, 114004. [[CrossRef](#)]

Disclaimer/Publisher's Note: The statements, opinions and data contained in all publications are solely those of the individual author(s) and contributor(s) and not of MDPI and/or the editor(s). MDPI and/or the editor(s) disclaim responsibility for any injury to people or property resulting from any ideas, methods, instructions or products referred to in the content.